SRNL-STI-2010-00509

CORROSION TESTING IN SIMULATED TANK SOLUTIONS

Elizabeth N. Hoffman

SEPTEMBER 2010

Savannah River National Laboratory
Savannah River Nuclear Solutions
Aiken, SC 29808

Prepared for the U.S. Department of Energy Under Contract Number DE-AC09-08SR22470

SRNL
SAVANNAH RIVER NATIONAL LABORATORY

DISCLAIMER

Printed in the United States of America

Prepared for
U.S. Department of Energy

SRNL-STI-2010-00509

Key Words:
Corrosion
Pitting

Retention:
Permanent

CORROSION TESTING IN SIMULATED TANK SOLUTIONS

Elizabeth N. Hoffman

SEPTEMBER 2010

Savannah River National Laboratory
Savannah River Nuclear Solutions
Savannah River Site
Aiken, SC 29808

Prepared for the U.S. Department of Energy Under Contract Number DE-AC09-08SR22470

REVIEWS AND APPROVALS

E.N. Hoffman, Co-author, Materials Performance & Corrosion Technology, SRNL Date

B.J. Wiersma, Technical Reviewer, Material Performance & Corrosion Technology, SRNL Date

K.E. Zeigler, Manager, Material Performance & Corrosion Technology, SRNL Date

K.D. Boomer, Program Manager, Washington River Protection Solutions Date

J.L. Castleberry, Project Manager for Double Shell Tank Integrity Project and Single Shell Tank Integrity Project, Washington River Protection Solutions Date

LIST OF ACRONYMS

CPP	Cyclic Potentiodynamic Polarization
PNNL	Pacific Northwest National Laboratory
RDE	Rotating Disc Electrode
SEM	Scanning Electron Microscope
SRNL	Savannah River National Laboratory

1.0 EXECUTIVE SUMMARY

Three simulated waste solutions representing wastes from tanks SY-102 (high nitrate, modified to exceed guidance limits), AN-107, and AY-102 were supplied by PNNL. Out of the three solutions tested, both optical and electrochemical results show that carbon steel samples corroded much faster in SY-102 (high nitrate) than in the other two solutions with lower ratios of nitrate to nitrite. The effect of the surface preparation was not as strong as the effect of solution chemistry. In areas with pristine mill-scale surface, no corrosion occurred even in the SY-102 (high nitrate) solution, however, corrosion occurred in the areas where the mill-scale was damaged or flaked off due to machining.

2.0 INTRODUCTION

Localized corrosion in the form of pitting in the vapor space of tank walls is an ongoing challenge to overcome in maintaining the structural integrity of the liquid waste tanks at the Savannah River and Hanford Sites. It has been shown that the liquid waste condensate chemistry influences the amount of corrosion that occurs along the walls of the storage tanks. To minimize pitting corrosion, an effort is underway to gain an understanding of the pitting response in various simulated waste solutions. Electrochemical testing has been used as an accelerated tool in the investigation of pitting corrosion. [1]

While significant effort has been undertaken to evaluate the pitting susceptibility of carbon steel in various simulated waste solutions, additional effort is needed to evaluate the effect of liquid waste supernates from six Hanford Site tanks (AY-101, AY-102, AN-102, AN-107, SY-102 (high Cl^-), and SY-102 (high nitrate)) on carbon steel. Solutions were formulated at PNNL to replicate tank conditions, and in the case of SY-102, exceed Cl^- and NO_3^- conditions, respectively, to provide a contrast between in and out of specification limits.

The majority of previous testing has been performed on pristine polished samples. To evaluate the actual tank carbon steel surface, efforts are needed to compare the polished surfaces to corroded and mill-scale surfaces, which are more likely to occur in application. Additionally, due to the change in liquid waste levels within the tanks, salt deposits are highly likely to be present along the tank wall. When the level of the tank decreases, a salt deposit will form as the solution evaporates. The effects of this pre-existing salt, or supernate deposit, are unknown at this time on the corrosion effect and thus require investigation.

Additionally, in the presence of radiation, moist air undergoes radiolysis [2, 3], forming a corrosive nitric acid condensate. This condensate could accelerate the corrosion process in the vapor space. To investigate this process, an experimental apparatus simulating the effects of radiation was designed and constructed to provide gamma irradiation while coupons are exposed to a simulate tank solution. Additionally, ammonia vapors will also be introduced to further represent the tank environment.

3.0 EXPERIMENTAL

3.1 EFFORT 1: ELECTROCHEMICAL TESTING USING SIMULATED TANK SOLUTIONS

Prior to electrochemical testing, samples were characterized using X-ray diffraction and SEM/EDS with particular focus on the corrosion-scale and mill-scale.

To minimize simulant usage, a BASi RDE-2 (rotating disc electrode) instrument was used for electrochemical testing with the sample rotation capabilities disabled. The RDE-2 setup requires ~20 ml of solution per run. Due to the small amount of solution required, the sample and electrodes are also miniaturized. Electrochemical cyclic potentiodynamic polarization testing was performed on 3.00 mm diameter ASTM A537 carbon steel tapped into mounting blanks. All testing was performed at 40 ºC in solution with air in the vapor space above the solution. A platinum mesh counter electrode and an Ag/AgCl reference electrode connected to a Luggin bridge were used in the cyclic potentiodynamic polarization testing. The potential was increased at 0.5 mV/sec up to a current density of $1.0x10^{-4}$ Amps/cm^2. Runs were terminated when the reverse potential equaled the original open circuit potential.

Cyclic potentiodyanmic polarization testing was performed on A537 carbon steel in bulk solutions simulating vapor space supernates supplied by EMSL (A. Felmy). In particular, the testing focused on:

1) The effect of the pre-existing surface layer (corroded, mill-scale, or polished) on pitting susceptibly in A537 carbon steel.
2) The effect of supernate deposits susceptibility in A537 carbon steel.

Coupons of A537 carbon steel were used with surfaces of:

1) Mill-scale (actual mill-scale direct from manufacturer's processing)
2) Corroded (corroded during storage via exposure to laboratory atmosphere)
3) Polished, 800 SiC grit
4) Pre-salt on Polished, 800 SiC grit

The compositions of the supplied simulants are listed in Tables 1-3.

Table 1 SY 102 data from 2/4/2004 (high NO3), pH=9.90

	Molarity	Salt compound	Molarity	MW (g)	Mass (g) for 1L
Na^{+1}	4.641		4.641		
Al^{+3}	0.069	$NaAlO_2$	0.069	81.97	5.659
K^{+1}	0.001	$KHCO_3$	0.001	100.114	0.056
Br^{-1}	0.074	NaBr	0.074	102.89	7.581
Cl^{-1}	0.013	NaCl	0.013	58.44	0.747
CrO_4^{-2}	0.011	Na_2CrO_4 $4H_2O$	0.011	161.97	1.833

F^{-1}	0.003	NaF	0.003	41.99	0.137
NO_3^{-1}	4.215	$NaNO_3$	4.215	84.99	358.255
NO_2^{-1}	0.112	$NaNO_2$	0.112	69.00	7.722
PO_4^{-3}	0.028	Na_3PO_4 x $12H_2O$	0.028	380.10	10.519
SO_4^{-2}	0.054	Na_2SO_4	0.054	142.05	7.681
Inorganic C	0.198	Na_2CO_3	0.200	105.99	21.198
		$NaHCO_3$	0.190	84.006	15.96

Table 2 AY102 data from 3/28/05, pH= 10.24

	Molarity	Salt compound	Molarity	MW (g)	Mass (g) for 1L
Na^{+1}	1.250		1.250		
K^{+1}	0.004	$KHCO_3$	0.004	100.114	0.37
Al^{+3}	0.021	$NaAlO_2$	0.021	81.97	1.74
Br^{-1}	0.015	NaBr	0.015	102.89	1.55
Cl^{-1}	0.001	NaCl	0.001	58.44	0.08
CrO_4^{-2}	0.000	Na_2CrO_4 $4H_2O$	0.000	161.97	0.01
F^{-1}	0.001	NaF	0.001	41.99	0.05
NO_3^{-1}	0.004	$NaNO_3$	0.004	84.99	0.34
NO_2^{-1}	0.296	$NaNO_2$	0.296	69.00	20.40
PO_4^{-3}	0.011	Na_3PO_4 x $12H_2O$	0.011	380.10	4.27
SO_4^{-2}	0.008	Na_2SO_4	0.008	142.05	1.07
Inorganic C	0.405	Na_2CO_3	0.370	105.99	39.22
		$NaHCO_3$	0.130	84.006	10.92

Table 3 241-AN-107 data from 2/18/2003 (latest data is 06/19/03 no OH), pH=10.40

	Molarity	Salt compound	Molarity	MW (g)	Mass (g) for 1L
Na^{+1}	8.758		8.758		
Al^{+3}	0.043	$NaAlO_2$	0.043	81.97	3.51
K^{+1}	0.045	KOH	0.045	56.11	2.55
Br^{-1}	0.037	NaBr	0.037	102.89	3.81
Cl^{-1}	0.051	NaCl	0.051	58.44	3.00
CrO_4^{-2}	0.003	Na_2CrO_4 $4H_2O$	0.003	161.97	0.55
F^{-1}	0.016	NaF	0.016	41.99	0.68
NO_3^{-1}	3.469	$NaNO_3$	3.469	84.99	294.82
NO_2^{-1}	1.492	$NaNO_2$	1.492	69.00	102.93
PO_4^{-3}	0.029	Na_3PO_4 x $12H_2O$	0.029	380.10	11.02
SO_4^{-2}	0.088	Na_2SO_4	0.088	142.05	12.51
Inorganic C	1.259	Na_2CO_3	1.260	105.99	133.40
		$NaHCO_3$	0.540	84.006	45.36

In the testing involving a pre-salt coverage prior to electrochemical testing, the samples were dipped into the electrolyte, then raised and dried to completion. Once a dried, hardened salt deposit was present on the sample, then the sample was lowered into the electrolyte and the open circuit potential determination was immediately started.

Post-electrochemical testing, samples were submersed in Clark's solution and placed in an ultrasonicator for 2 minutes to remove corrosion product to expose surface damage. After sonication, the samples were rinsed with distilled water. Optical images were captured of the sample surface. Select samples were sent to EMSL for additional characterization using the focused-ion beam and micro-XRD.

3.2 EFFORT 2: SIMULATED RADIATION ENVIRONMENT VESSEL DESIGN

It is known that nitric acid forms as a result of the irradiation of moist air. The formation of a nitric acid vapor, followed by deposition onto the tank wall will accelerate corrosion in the vapor space region.

The objective of this effort is to design and test a vessel to provide a simulated radiation environment resulting in the formation of a nitric acid condensate depositing onto metallic coupons representing the tank wall. This work will develop the experimental apparatus to be utilized in interval coupon testing for investigations into solution and salt interaction in a radiological environment and the resulting corrosion that forms. Additionally, the effects of carbon dioxide and ammonia gas in the vapor space will be evaluated.

4.0 RESULTS

4.1 ELECTROCHEMCAL TESTING

4.1.1 Pre-electrochemcal testing

The X-ray diffraction results of the mill-scale and corroded surfaces of the A537 carbon steel were similar; with the exception that wustite (FeO) was detected on the corroded surface. Both surfaces contained hematite (Fe_2O_3), iron (Fe), and magnetite (Fe_3O_4), see Figures 1 and 2). Table 4 lists the highest intensity peaks for each compound identified.

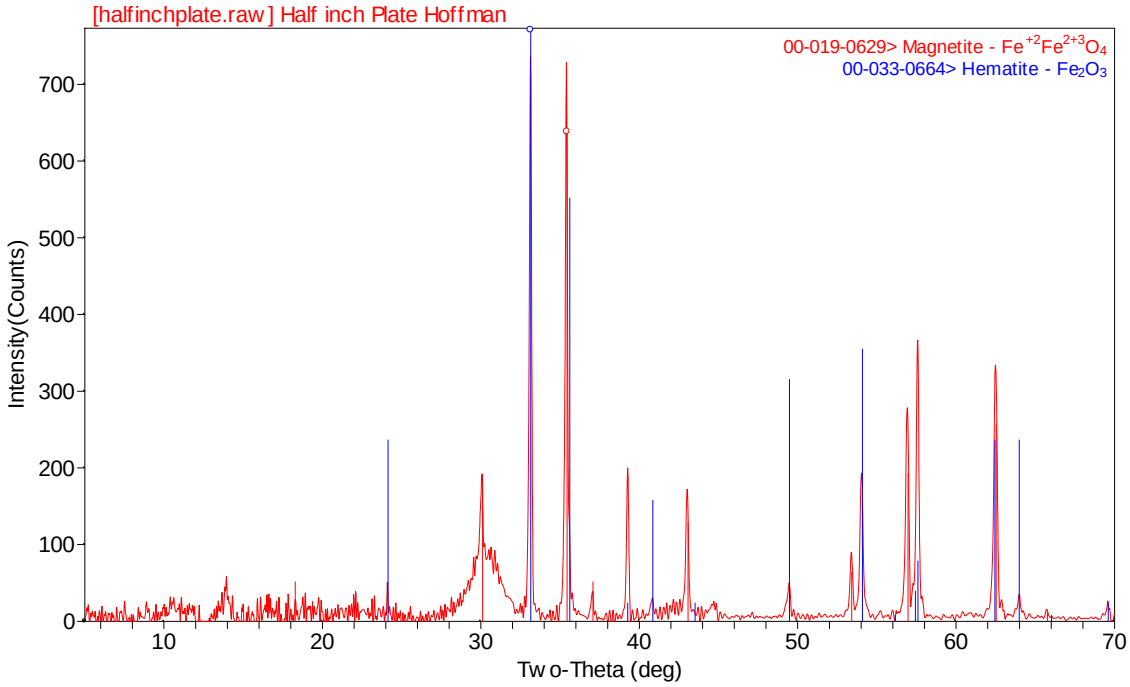

Figure 1: X-ray diffraction of mill-scale surface of A537 carbon steel.

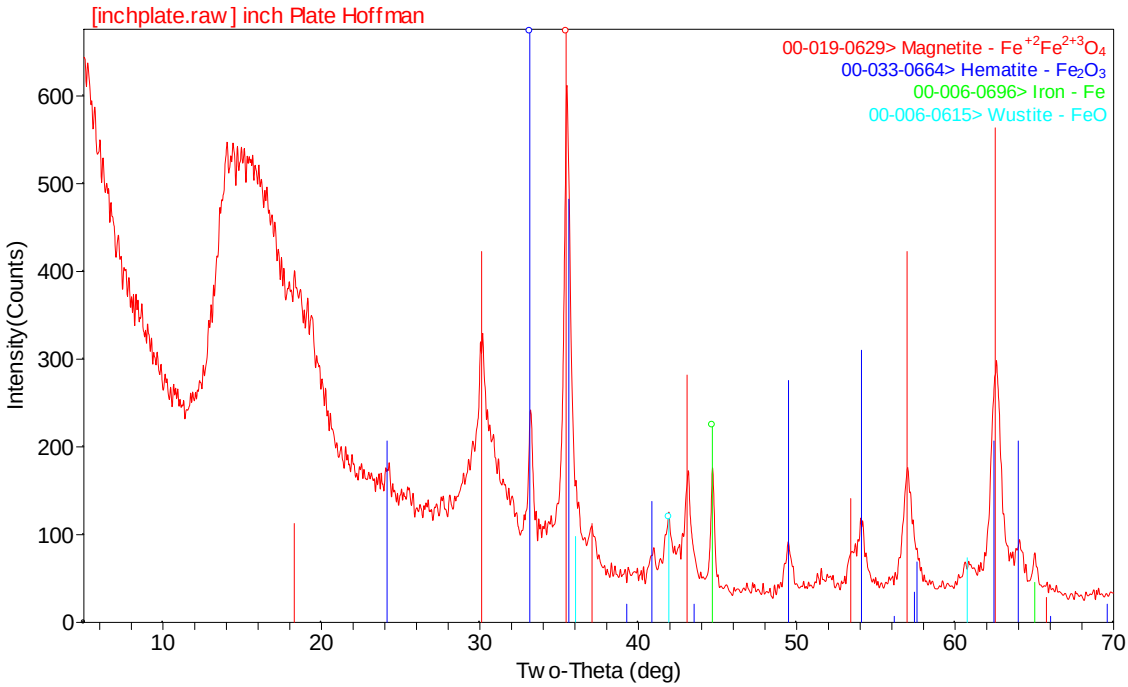

Figure 2: X-ray diffraction of corroded surface of A537 carbon steel.

Table 4 Listing of four highest intensity X-ray diffraction peaks for identified compounds. Values are listed in 2θ in order of decreasing intensity.

Magnetite (Fe_2O_4)	Hematite (Fe_2O_3)	Iron (Fe)	Wustite (FeO)
35.423	33.153	44.674	41.928
62.516	35.612	82.334	36.041
56.944	54.090	65.022	60.766
30.095	49.480	116.389	72.739

Scanning electron micrographs show a more distinctive difference between the mill-scale and corroded surfaces. The mill-scale surface, shown in Figure 3, contains a more homogeneous oxide compared to the corroded surface, shown in Figure 4. Additionally, the micrograph shows that for the mill-scale surface, the actual mill-scale flaked off at the edges upon electro-discharge machining (EDM). This result indicates that the mill-scale, particularly at edges, is fragile, and can be damaged through machining.

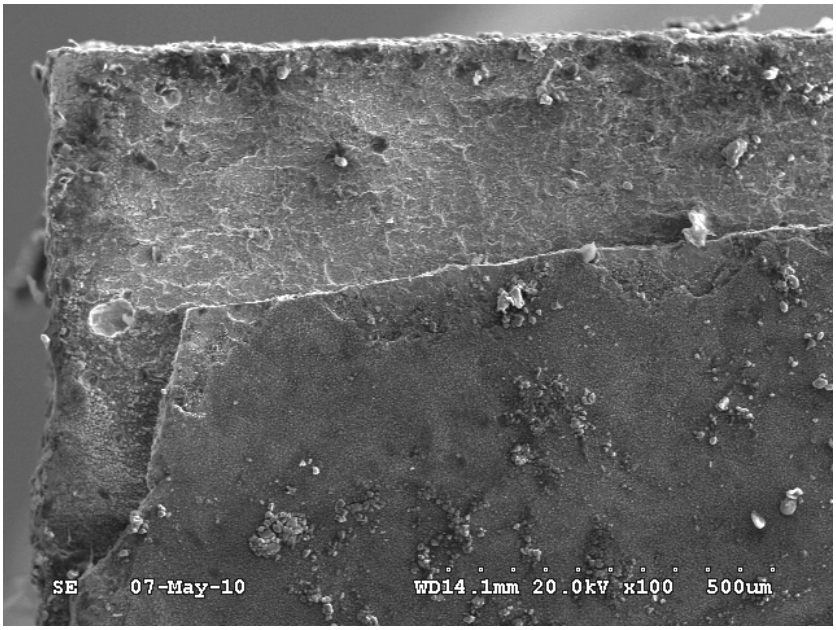

Figure 3 Mill-scale surface prior to electrochemical testing. Note, mill-scale was damaged during machining. No scale is present at the upper portion of the image.

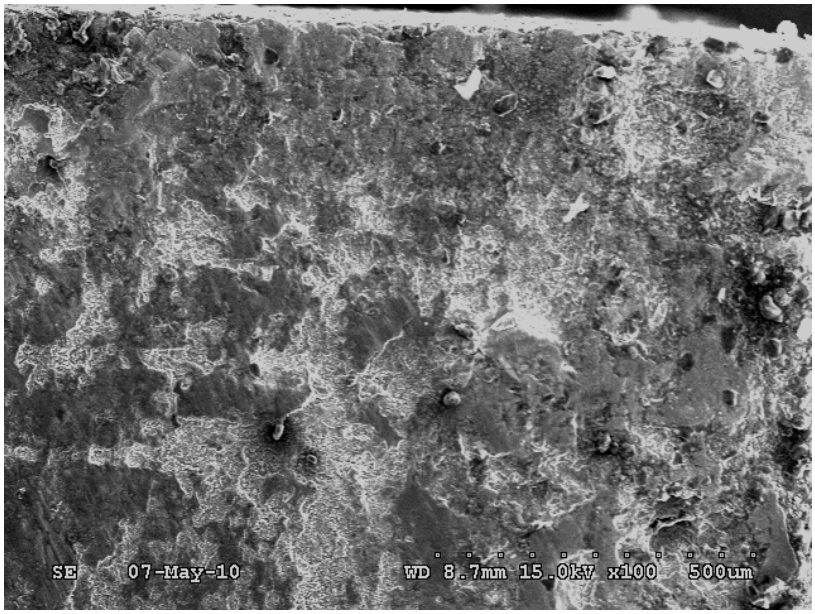

Figure 4 Corroded surface of A537 carbon steel prior to testing.

4.1.2 CPP Curves and Corresponding Optical Images

Cyclic potentiodynamic polarization results and corresponding optical images of the polished surfaces using SY-102 (high nitrate), AN-107, and AY-102 as electrolytes are shown in Figures 5, 6, and 7. The SY-102 (high nitrate) solution resulted in significant corrosion of the sample as shown by the optical images. The CPP curve supports this result with a positive hysteresis. The other two solutions, AN-107 and AY-102, did not result in a corrosive response and the CPP curve supports this result with a negative hysteresis.

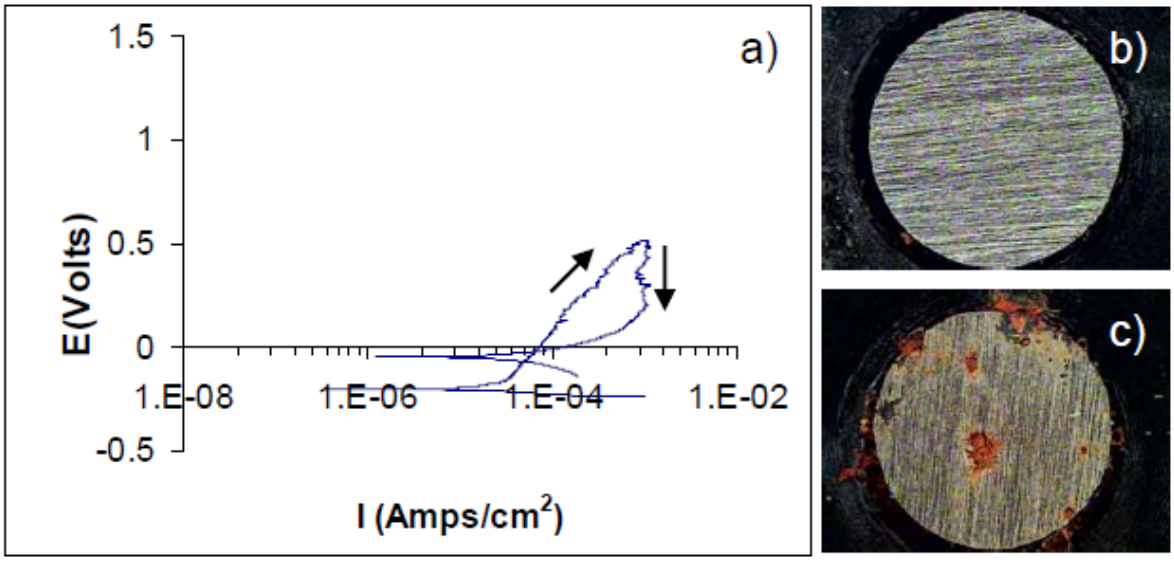

Figure 5: Polished sample tested in SY-102 (high nitrate) electrolyte: a) CPP curve, b) before electrochemical testing, c) after electrochemical testing

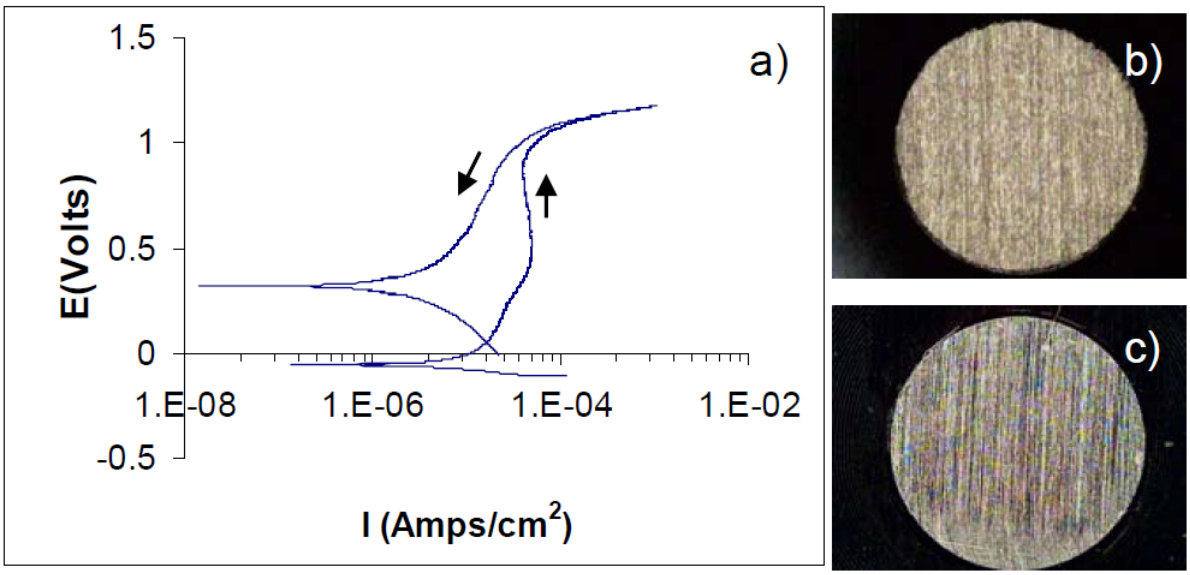

Figure 6: Polished sample tested in AN-107 electrolyte: a) CPP curve, b) before electrochemical testing, c) after electrochemical testing

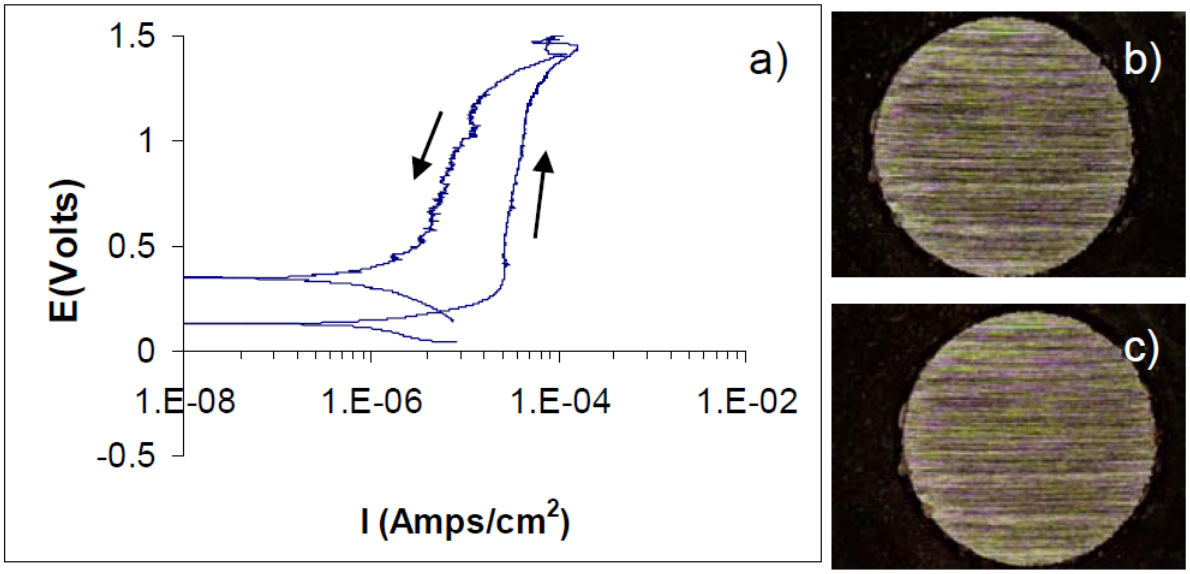

Figure 7: Polished sample tested in AY-102 electrolyte: a) CPP curve, b) before electrochemical testing, c) after electrochemical testing

A clearer breakdown potential was measured in the CPP curve and less obvious crevice attack was observed on the coupon for the pre-salt SY-102 (high nitrate) compared to the polished surface alone, see Figure 8. In solutions AN-107 and AY-102, the addition of a pre-

salt on the polished surface did not result in a large difference in CPP and optical images, see Figures 9 and 10.

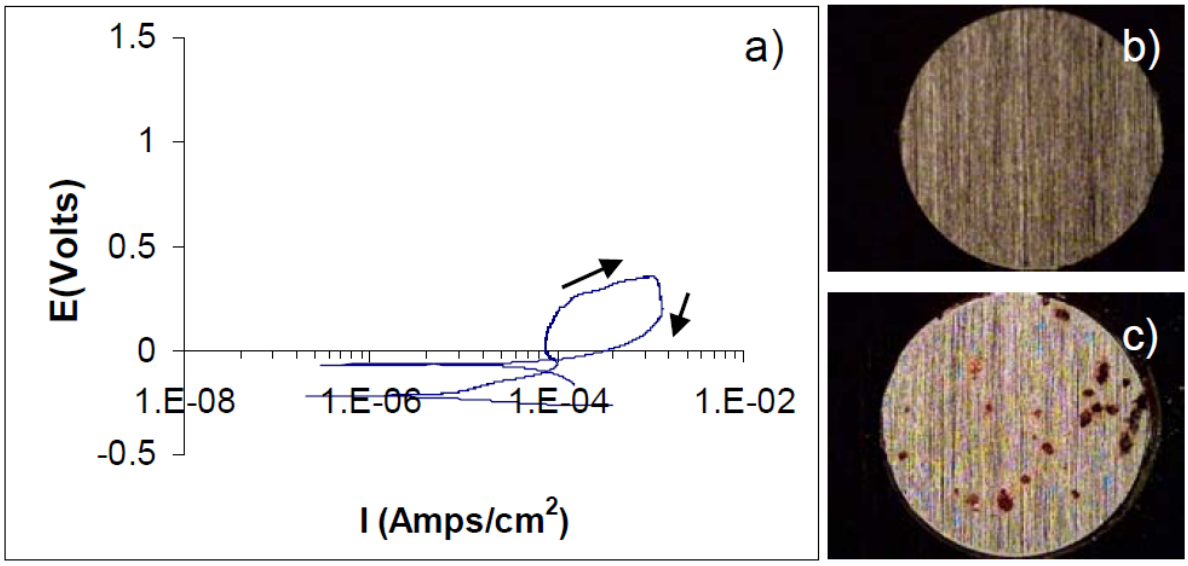

Figure 8: Polished with pre-salt sample tested in SY-102 (high nitrate) electrolyte: a) CPP curve, b) before electrochemical testing, c) after electrochemical testing

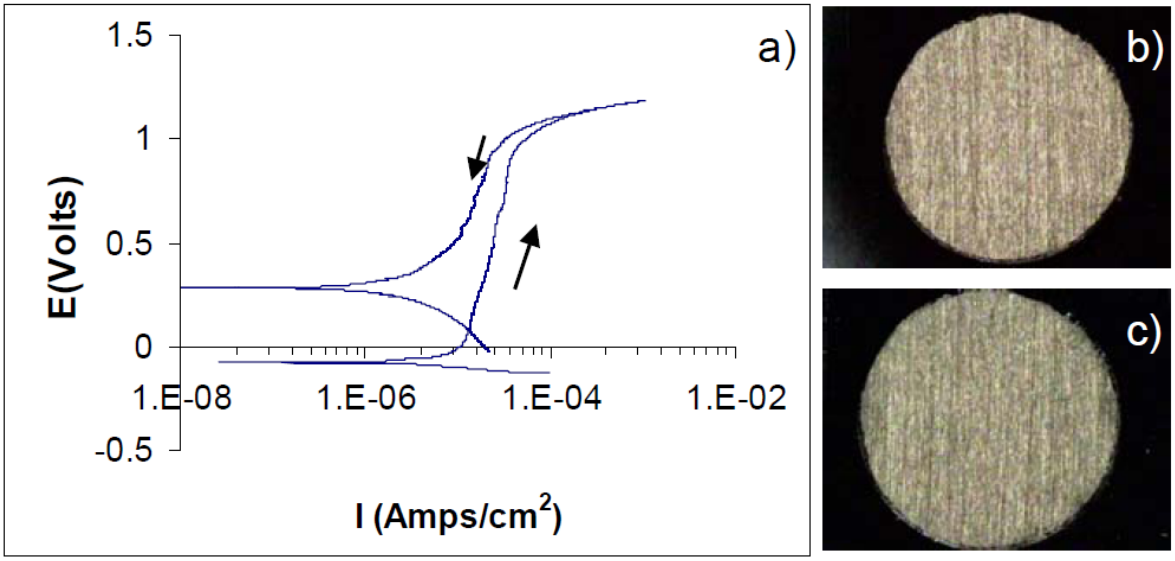

Figure 9: Polished with pre-salt sample tested in AN-107 electrolyte: a) CPP curve, b) before electrochemical testing, c) after electrochemical testing

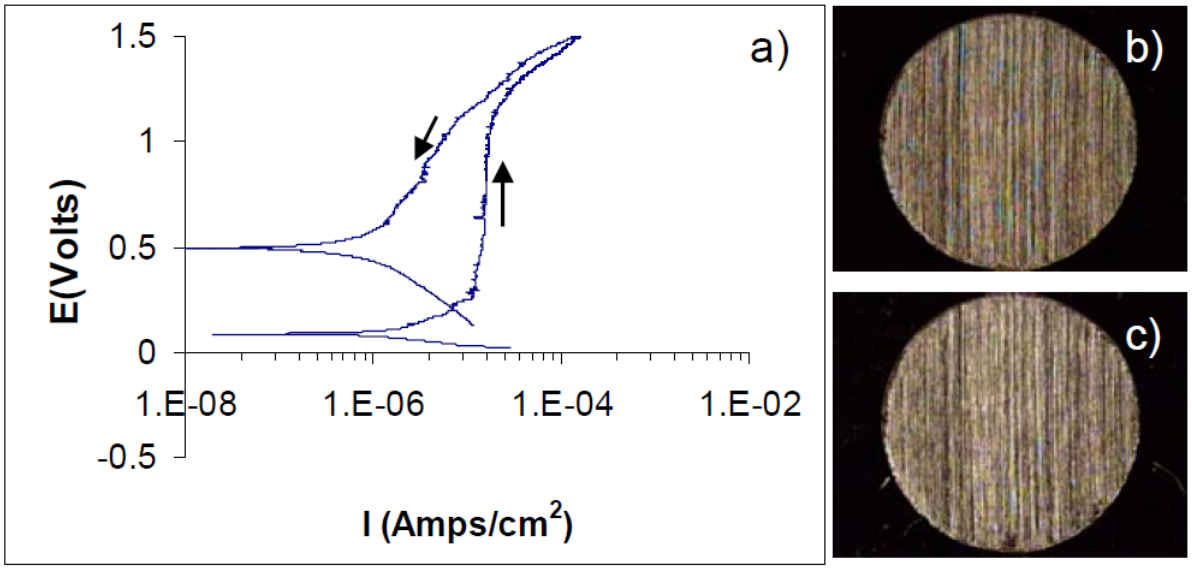

Figure 10: Polished with pre-salt sample tested in AY-102 electrolyte: a) CPP curve, b) before electrochemical testing, c) after electrochemical testing

When testing with a corroded surface, again, the SY-102 solution is the only solution that results in considerable corrosion, see Figures 11, 12, and 13. A significant portion of corrosion occurred in the form of edge attack, Figure 11. A537 samples were tapped into polymeric mounts with a pre-existing hole. Care was taken to level the surface of the blank with the surface of the metal sample; however, it was not possible to completely eliminate the height difference between the surfaces without disturbing the surface condition. In the case of SY-102 (high nitrate), the difference between the blank surface and the plastic surface was 0.0055". Caution should be used when taking the edge corrosion into account as it most likely was initiated at the machined surface.

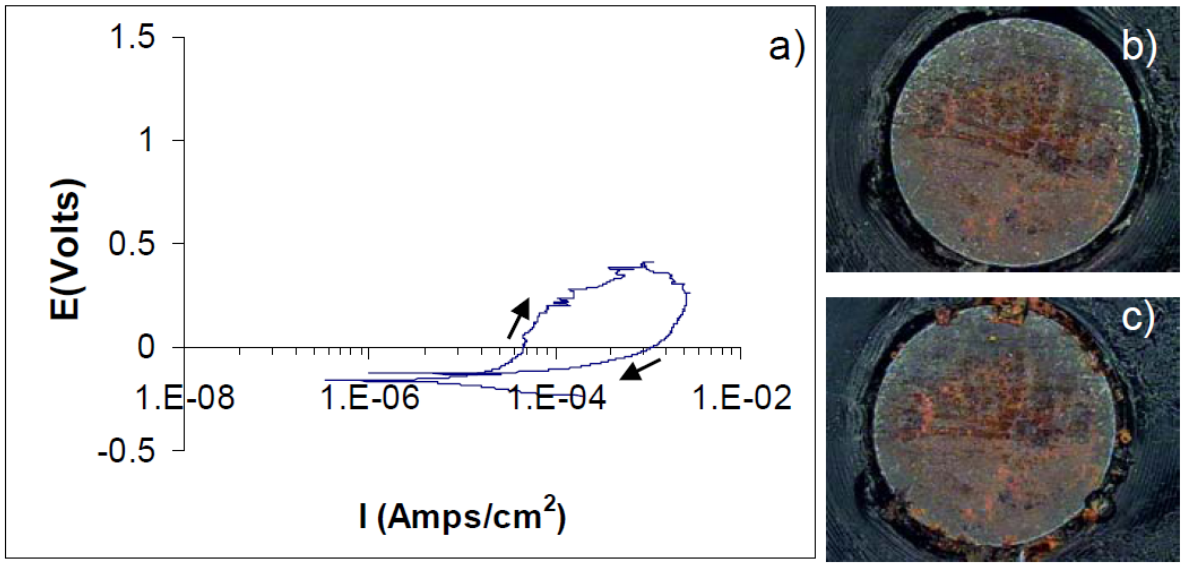

Figure 11: Corroded sample tested in SY-102 (high nitrate) electrolyte: a) CPP curve, b) before electrochemical testing, c) after electrochemical testing

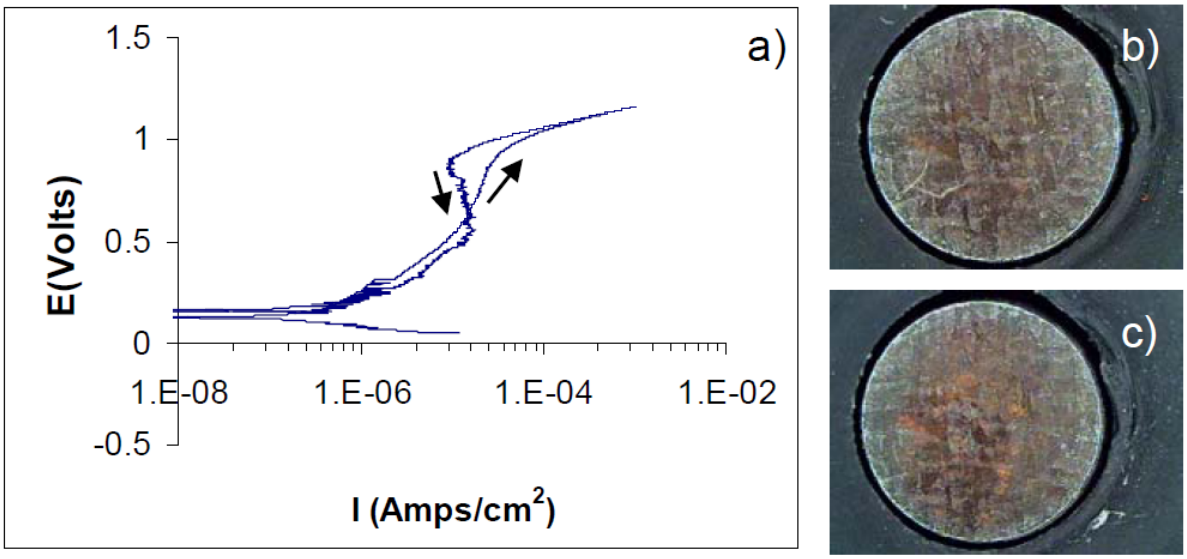

Figure 12: Corroded sample tested in AN-107 electrolyte: a) CPP curve, b) before electrochemical testing, c) after electrochemical testing

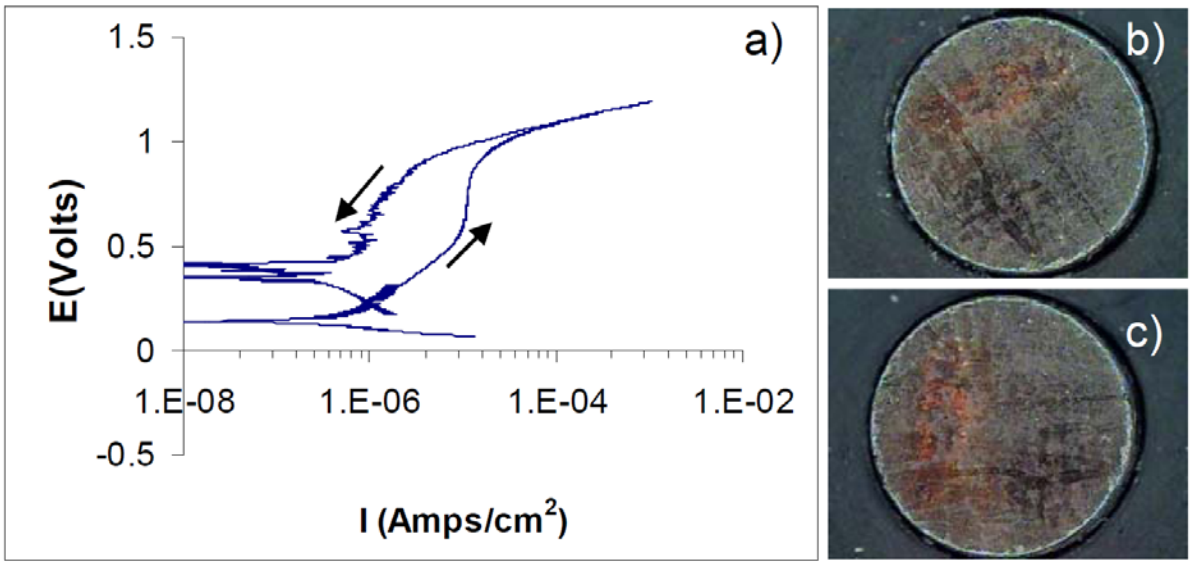

Figure 13: Corroded sample tested in AY-102 electrolyte: a) CPP curve, b) before electrochemical testing, c) after electrochemical testing

In the case of the mill-scale surface, samples exposed to SY-102 (high nitrate) corroded only in areas that were not covered by mill-scale: at the mill-scale edge and exposed machined surface due to the height difference between the sample and the plastic blank. In the case of SY-102 (high nitrate), the difference was 0.014". The sample exposed to solution AN-107 resulted in a positive hysteresis, however, no evidence of corrosion was found on the optical image after testing. See Figures 14, 15, and 16 for results.

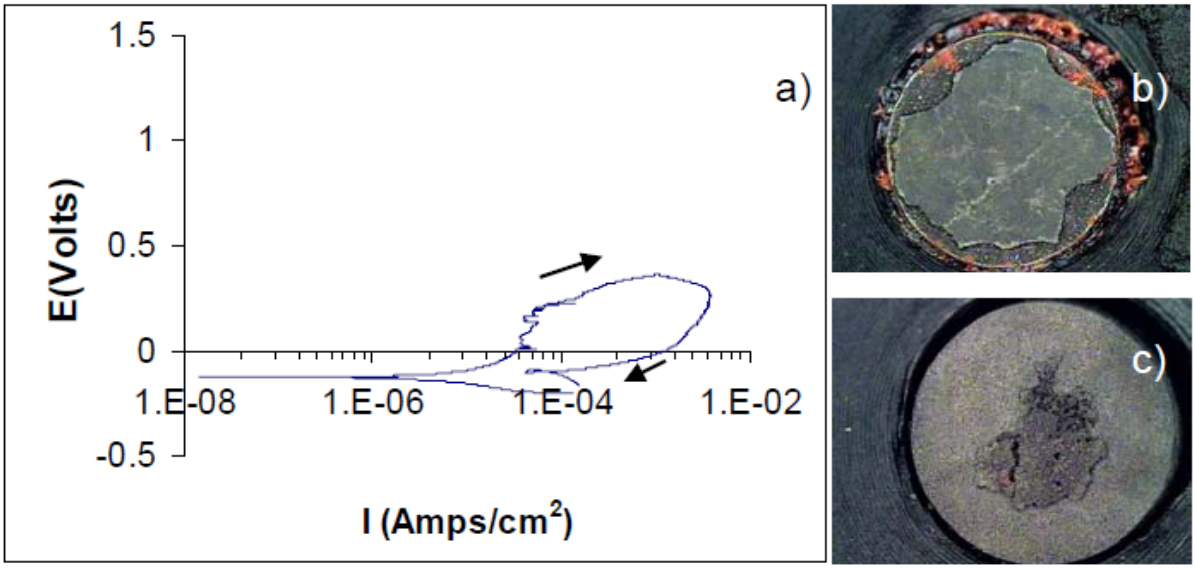

Figure 14: Mill-scale surface sample tested in SY-102 (high nitrate) electrolyte: a) CPP curve, b) after electrochemical testing, c) after cleaning.

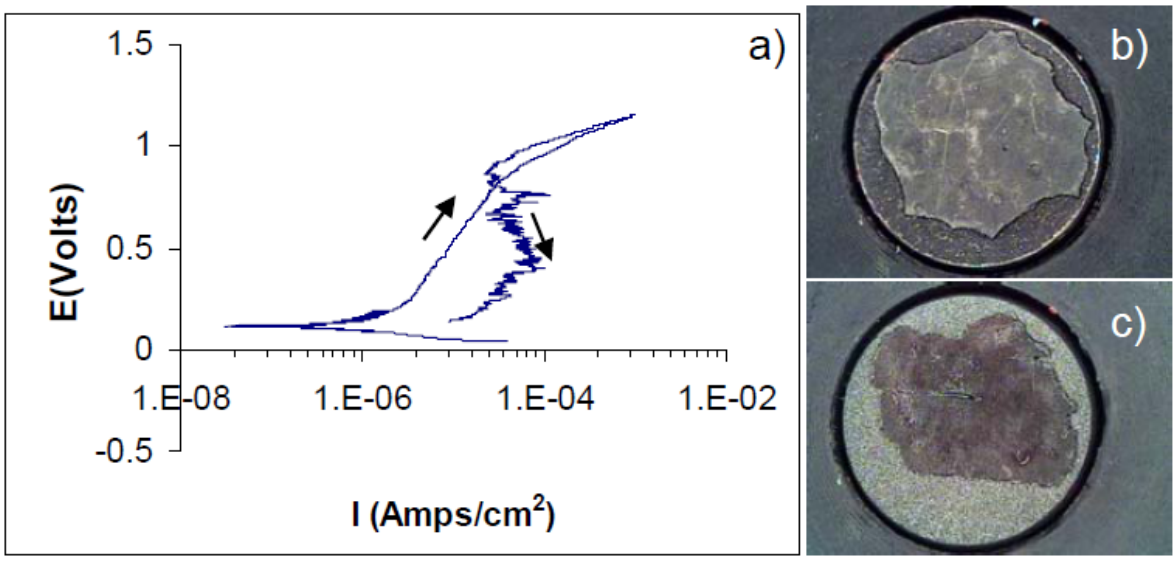

Figure 15: Mill-scale surface sample tested in AN-107 electrolyte: a) CPP curve, b) after electrochemical testing, c) after electrochemical cleaning.

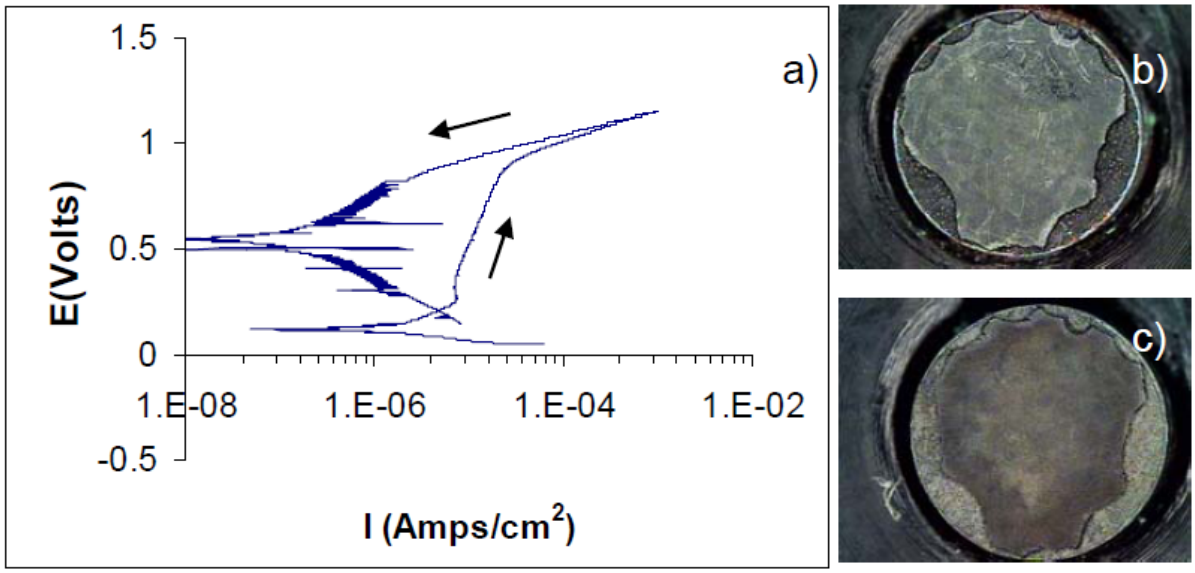

Figure 16: Mill-scale surface sample tested in AY-102 electrolyte: a) CPP curve, b) before electrochemical testing, c) after electrochemical testing

Solution SY-102 (high nitrate) was the only solution that resulted in repassivation during the reverse scan, see Table 5. Of the SY-102 (high nitrate) solutions, only the mill-scale condition did not result in a repassivation potential, E_{rp}. Values for E_{rp} ranged from -0.028 to -0.129 V for the polished and corroded surfaces, respectively. The transpassive potential, E_{trans}, was within 300 mV of 1.0 V for solutions AN-107 and AY-102. Solution SY-102 (high nitrate) measured lower pitting potentials, E_{pit}, ranging from 0.280 V for the corroded surface to 0.449 V for the polished surface.

Table 5 Electrochemical parameters, E_{cor}, E_{pit}, E_{trans} and E_{rp}, based on electrochemical scans. Note, E_{pit} pertains to SY-102 (high nitrate solutions), E_{trans} pertains to AN-107 and AY-102 solutions.

Solution	Sample Surface	E_{cor} (V)	E_{pit} or E_{trans} (V)	E_{rp} (V)
AN-107	Corroded	0.126	0.961	--
AN-107	Polished	-0.053	0.990	--
AN-107	Polished with Pre-salt	-0.074	1.005	--
AN-107	Mill-scale	0.125	0.920	--
AY-102	Corroded	0.152	0.935	--
AY-102	Polished	0.127	1.287	--
AY-102	Polished with Pre-salt	0.089	1.169	--
AY-102	Mill-scale	0.119	0.925	--
SY-102 (high nitrate)	Corroded	-0.161	0.280	-0.129
SY-102 (high nitrate)	Polished	-0.205	0.449	-0.028
SY-102 (high nitrate)	Polished with Pre-salt	-0.222	0.272	-0.047
SY-102 (high nitrate)	Mill-scale	-0.123	0.304	--

Due to the break-off of mill-scale from the machining process, the reproducibility of the mill-scale CPP curves was evaluated by running multiple mill-scale surface samples. It was found that the reproducibility of the CPP curves was on the order of +/-150 mV. This result is consistent with runs using polished surface samples.

4.2 SIMULATED RADIATION VESSEL

A glass vessel capable of holding 3 liters of solution has been designed and fabricated, see Figure 17. The vessel creates a simulated radiation environment by providing a nitric acid vapor environment. Additionally, the vessel has the flexibility to also provide a nitric acid and ammonia vapor environment via a connection to a gas mixture of 20 ppm NO_2 and 50 ppm NH_3. A salt solution will be added to the vessel to control the relative humidity based on ASTM E104-02. Corrosion samples can be suspended from two different rods at two different levels within the vapor space. The rods and sample spacers are made from Teflon to prevent galvanic corrosion.

Figure 17: The simulated radiation environment vessel equipped with two Teflon hanging rods, ports for gas inlet and outlet, a safety pressure relief plug, and optional solution bubbler.

5.0 DISCUSSION

Based on both cyclic potentiodynamic polarization curves and corresponding optical image results, the solution SY-102 is considerably more corrosive than the AY-102 and AN-107 solutions. The major difference in the solutions is that the SY-102 (high nitrate) solution has more nitrate, 4.215 M molarity, compared to the other two solutions, 0.004 M and 3.469 M, respectively, see Tables 1-3. When the ratio of nitrate to nitrite (aggressor to inhibitor species) per solution is calculated, the difference between the SY-102 (high nitrate) solution

and the other two solutions is further magnified. The ratio of NO_2/NO_3 for the SY-102 (high nitrate) solution is 0.026 versus 100 and 0.431 for the AY-102 and AN-107, respectively. AY-102 is not a nitrate-ion waste, but a carbonate-ion waste, which yields a significantly higher NO_2/NO_3 ratio compared to AN-107 and SY-102 (high nitrate).

The effect of the surface condition prior to testing did not play as large of a role compared to the solution chemistry of the electrolyte used. The pre-salt formed directly from the testing solution did not result in a significant change in the electrochemical response. The corroded surface also did not play a significant role in affecting the corrosion response. While the mill-scale surface, did not result in a significant change in the corrosion response compared to the polished surface, it did yield results of interest when comparing the optical images before and after cleaning with Clark's solution. Corrosion at the edge of the mill-scale appeared to occur in the SY-102 (high nitrate) solution, see Figure 14b. After cleaning all three mill-scale samples with Clark's solution, a higher percentage of mill-scale on the SY-102 (high nitrate) sample was removed due to the cleaning process, see Figure 14c. The sample with the least mill-scale loss was AY-102, which also had the lowest ratio of NO_3/NO_2. The loss of mill-scale on the samples is most likely due to a corrosive attack occurring at the edge of the mill-scale, then spreading to under the mill-scale. This reaction could have resulted in the breakdown of the mill-scale adhesion to the sample surface. Therefore, while mill-scale itself is protective against corrosion, when exposed to a corrosive solution, the scale can be compromised through crevice attack.

6.0 CONCLUSIONS

Out of three solutions tested, both optical and electrochemical results show that carbon steel corroded much faster in SY-102 (high nitrate) compared to the other two solutions, AN-107 and AY-102, with lower ratios of nitrate to nitrite. The effect of the surface preparation was not as strong as the effect of solution chemistry. In areas with pristine mill-scale surface, no corrosion occurred even in the SY-102 (high nitrate) solution, however, corrosion occurred in the areas where the mill-scale was damaged or flaked off due to machining.

7.0 REFERENCES

[1] Electrochemical Techniques in Corrosion Science and Engineering, R.G. Kelly, J.R. Scully, D.W. Shoesmith, R.G. Buchheit (2003) Taylor & Francis Group: Boca Raton

[2] Y. Kanda, T. Miura, H. Nakajima, *Radiation Physics and Chemistry* **77** [7] (2008) 884-888

[3] M. Terry, J. Beavers, G. Frankel, J. Huckaby, L. Stock, K. Subramanian, B. Wiersma, "Expert Panel Workshop on Double-Shell Tank Vapor Space Corrosion Testing", RPP-RPT-31129, (2006)